Bulgarian Society for NDT
International Journal "NDT Days"
Volume V, Issue 3, Year 2022
ISSN: 2603-4018
eISSN: 2603-4646

Microstructural and Mechanical Characterization of Non-linear Friction Stir Welded A 6061 Alloy

Christo KONDOFF[1], Radostina ZAEKOVA[1], Yasen HADJITODOROV[1], Rumen KRASTEV[2], Tatiana SIMEONOVA[1,2]

[1]Institute of Metal Science, equipment, and technologies with Center for Hydro- and Aerodynamics "Acad. A. Balevski" at the Bulgarian Academy of Sciences, Sofia, Bulgaria

[2]Institute of Mechanics at the Bulgarian Academy of Sciences, Sofia, Bulgaria

e-mails: hriko61@gmail.com, rzaekova@ims.bas.bg, jason@ims.bas.bg, krastev.sc@gmail.com, tsimeonova@imbm.bas.bg

Abstract
Friction stir welding is one of the fastest developing processes in the last thirty years. The list of materials for welding and processing by this technology is constantly growing. At the same time, the process is being developed and improved in order to increase productivity, the quality of welded joints and overcome its imperfections. In this investigation a friction stir welding, which is carried out by moving the working tool on a cycloid-like trajectory is presented. Depending on the direction of movement along the cycloid-like line, a boundary zone of one type "advanced side" or "retreated side" can be created. The results of metallographic and strength studies of welded joints realized with linear motion and cycloid-like trajectory are presented. An analysis of the results has been made and guidelines for further research have been outlined.

Keywords: Aluminium alloy A6061, friction stir welding (FSW), Tensile test, hardness, structure.

1. Introduction

Friction stir welding (FSW) and friction stir processing (FSP) find increasing application in automotive industry, shipbuilding, aerospace industry and other areas [1,2,3,4]. The processes take place in a plastic state without melting, using the heat released during friction, without the need for a welding power source, additional material, shielding gas and additional processing. In addition, the corrosive properties of the material do not deteriorate, no harmful gases are emitted and there is no harmful light radiation. The method is applied to almost all plastic materials and alloys and gives possibility to weld dissimilar materials. FSP makes it possible to modify certain surface areas of the product, resulting in formation of metal matrix composites. It is possible to improve the structure by introducing powders of different characteristics in order to achieve specific properties, such as increased hardness, wear resistance, corrosion resistance and others. [5,6,7,8].
The disadvantages of FSW and FSP are reduction of thickness in the treatment area, key hole defect resulting from the exit of the tool, metal deficient areas and areas without metallurgical bond between the layers due to insufficient rupture of the oxide layer because of poor combination of the parameters of the processing mode and the geometric characteristics of the tool [9]. To overcome these problems, different solutions have been introduced, such as improving both the FSW and FSP methods (with two oppositely working instruments (DS-FSW) [10], using ultrasound, applying underwater repeated processing, etc.), or subsequent heat treatment [11]. The so-called RT-type configuration for better oxide layer rupture has also been proposed [12]. It was found out [13] that during tensile testing of FSW samples of heat-treated aluminium alloys, the fracture always occurs on the retreated side. This is due to

the presence of a zone with reduced hardness at the boundary of TMAZ, which is wider than the one from the advanced side (fig. 1).

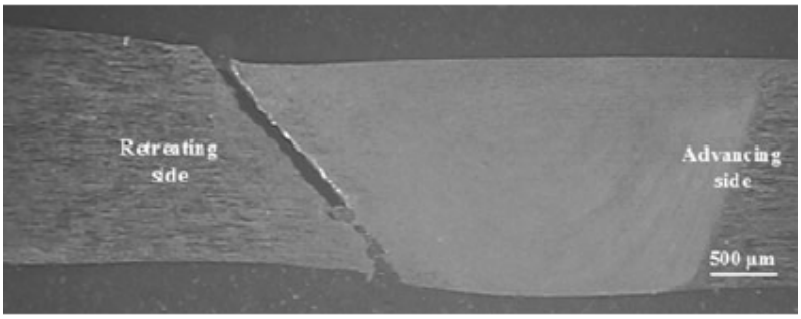

Fig.1. Fraction location of a typical FSW joint [13].

2. Problem analysis and solution proposal

The FSW and FSP methods are based on asymmetry due to the uni-directional rotation of the tool. On the advanced side, the directions of the velocity vector in the rotational movement of the tool and the velocity vector of the translational movement in the processing direction coincide. On the retreated side of the instrument, these two vectors are divergent.

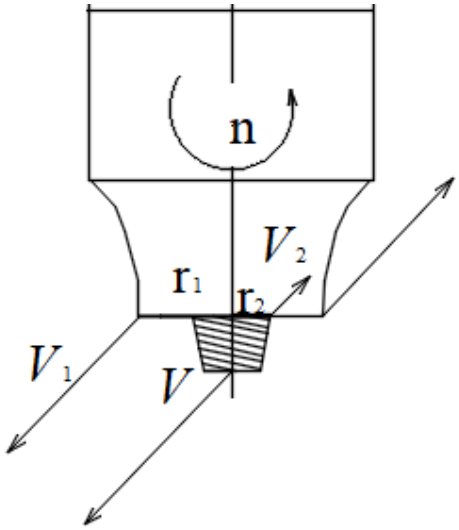

Fig.2. FSP tool

In order to assess the significance of the two velocities for the overall course of the process, we compare their magnitudes. The velocity of rotation of the tool is n [rpm]. The angular velocity is

$$\omega = \frac{\pi n}{30}[rad/s] \tag{1}$$

The peripheral velocity depends on the dimensions of the tool (Fig. 2). The diameter of the tool shoulder is 13 mm and the diameter of the pin at its base is 5.5 mm:

$$r_1 = 6.5[mm] = 6.5 \times 10^{-3}[m], \; r_2 = 2.25[mm] = 2.25 \times 10^{-3}[m]$$

The peripheral velocities of the shoulder and the pin are respectively

$$V_1 = \omega r_1[m/s], \; V_2 = \omega r_2[m/s] \tag{2}$$

In case the rotation speed n = 900 rpm:

$$\omega = \frac{\pi n}{30} = \frac{900\pi}{30} = 30\pi = 94.25[rad/s]$$

$$V_1 = \omega r_1[m/s]$$

$$V_1 = \omega r_1 = 94.25 \times 6.5 \times 10^{-3} = 0.6126[m/s]$$

$$V_2 = \omega r_2 = 94.25 \times 2.25 \times 10^{-3} = 0.212[m/s]$$

The linear velocity in translational motion V = 60 cm/min = 0.6 m/min = 0.01 m/s.

This result indicates that the velocity obtained as a result of the rotation of the tool $V_1/V = 0.6126/0.01 = 61.26$ and $V_2/V = 0.212/0.01 = 21.4$ is dominant.

In this case, the relative velocity of the tool and the velocity of movement of the processed material of the workpiece differ significantly depending on the distance of the envisaged point to the surface in contact with the shoulder. This speed is lowest at the root of the weld and it can be the cause of defects in this area.

Nevertheless, a pronounced asymmetry is observed in the texture of the mixed area (Fig.3).

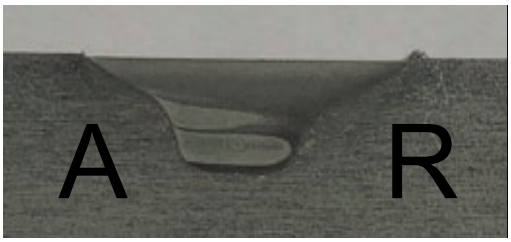

Fig.3. Macrostructure of the cross section of FSW of A 6061 in a single pass.

The boundary between the nugget zone and the raw material on the side of the tool entry A (advanced side) is sharper and more pronounced, while on the side of the exit R (retreated side) it is smoother. The light areas in the texture correspond to finer grains structure, while darker areas are mainly consisted of deformed structural grains. These prerequisites affect the properties of the material in the processed area.

It is possible to change the type of the boundary between the nugget zone and the unprocessed material if the tool performs additional movement on a non-rectilinear cycloid-like trajectory with deviation from the rectilinear axis of processing. Depending on the direction of rotation, boundaries type A or type R can be obtained.

3. Experimental procedure

Friction stir welding was performed on 2 pairs of A6061 T651 plates (1wt% Mg, 0.63wt% Si, 0.19wt% Cu, 0.06wt% Cr, 0.09wt% Mn, 0.31wt% Fe, 0.12wt% Zn and balance Al) with dimensions 200x100x12 mm. The tool has a concave shoulder with diameter 13 mm and a pin with threaded grooves on the surrounding surface and three grooves on the generating line with diameter 5.5 mm at the base. Processing center "Hurco" was used to perform FSW (Fig.4). Based on preliminary research, the review of publications on the topic and the

considerations of maximum productivity, the tool rotation speed of 900 rpm and a linear processing speed of 60 mm/min were selected.

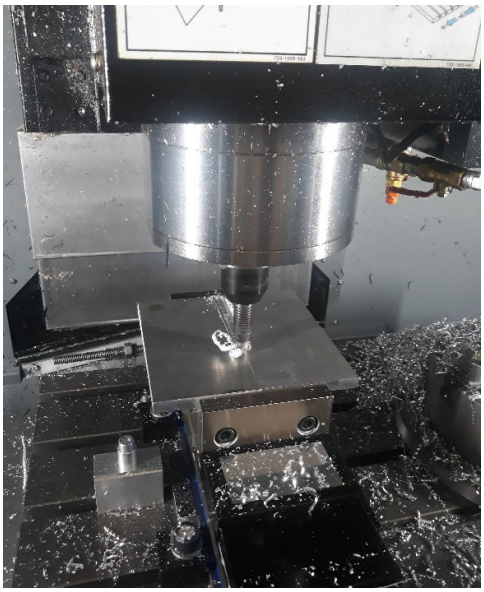

Fig.4. FSW on Hurco processing center

The first pair of plates are welded along a linear trajectory of tool transition and the second pair are welded along a cycloid-like trajectory with a deviation from the axis of 6 mm (Fig.5). Three series of specimens were prepared for tensile testing: specimens from the base material Al 6061 T651 marked as series “B”; rectilinearly welded specimens marked as series “V”; and specimens welded along cycloid-like trajectory of movement of the tool marked as series “S”.

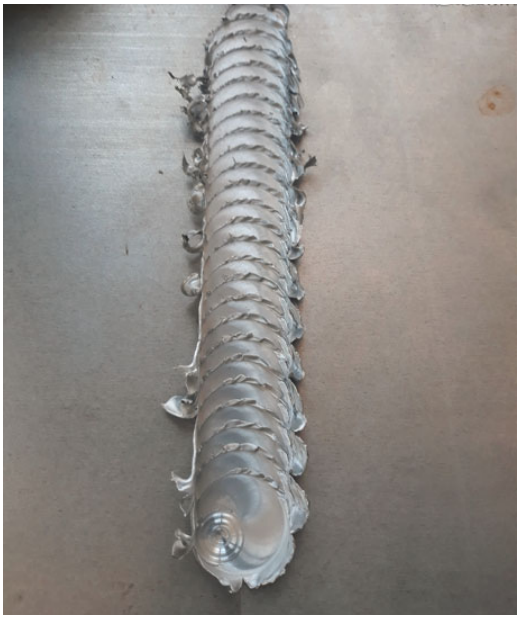

Fig.5. FSW along cycloid-like trajectory

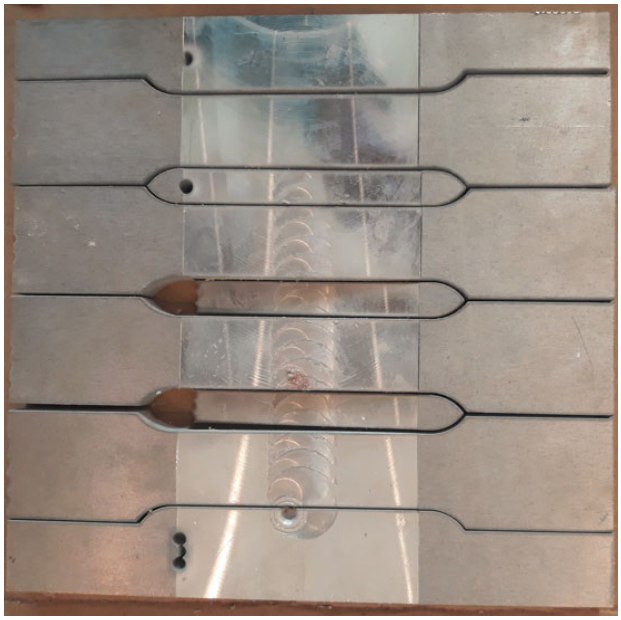

Fig.6. Cutting the samples

The specimens for tensile testing and metallographic analyses are cut on waterjet cutting machine (Fig.6).

4. Results and discussion

4.1. Metallographic analyses

The specimens for metallographic analyses of welds series “V” and “S” are made of the material located between the second and third tensile test specimens (Fig.6). The samples were processed and developed according to the standard procedure for this alloy. For a more detailed picture, a series of micro-photos were taken, which are united in a complete image. The samples of series “V” and “S” are shown in Fig. 7 and Fig. 8 respectively.

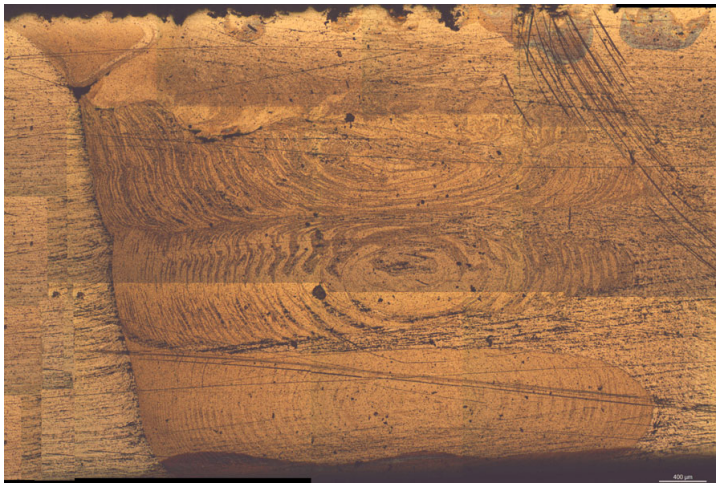

Fig.7. Microstructure image of the weld in rectilinear FSW, series “V”.

Fig.8. Microstructure image of the weld in FSW along cycloid-like trajectory, series “S”.

There is a sharp boundary in linear FSW (series “V”, Fig.7) between the stirred material and the base material on the advanced side (on the left) and characteristic root-like penetrations of the base material into the nugget zone (on the right). Separate metal deficiency zones can also be seen (Fig.7). There is symmetry on the left and right sides of the image of a weld in FSW on a cycloid-like trajectory (Fig. 8, series “S”). Here, too, there is a root-like penetration of the base metal and characteristic furrows.

4.2. Tensile testing

The tensile properties of the basic material and both of the tested series "V" and "S" are shown in table 1.

Table. 1 Tensile test properties

Property	Designation	Unit	Base material	Series "V"	Series "S"
Elastic modulus	E	GPa	71.2 ± 1.7	71.6 ± 2.6	71 ± 2.8
Proof strength	$R_{P0.2}$	MPa	279 ± 5	146 ± 21	95 ± 7
Ultimate tensile strength	R_m	MPa	310 ± 5	195 ± 8	161 ± 2
Fracture deformation	A_{25}	%	12.0 ± 0.8	7 ± 3	14 ± 2

The stress-strain diagrams obtained for both researched regimes are shown in fig. 9 and 10.

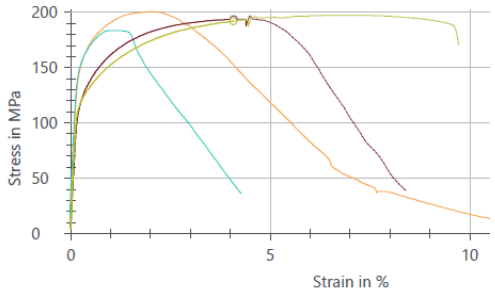

Fig. 9. Tensile testing of weld joints series "V"

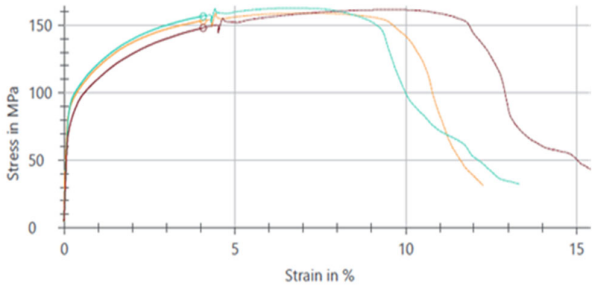

Fig. 10. Tensile testing of weld joints series "S"

Fig. 11 shows a comparison of selected diagrams that are representative of the mechanical tensile behavior of the base material (B), the weld joints obtained by rectilinear motion (V) of the tool and the weld joint obtained by a cycloid-like trajectory (S). As it can be seen, friction stir welded specimens possess lower tensile properties compared to the base material, which is due to the precipitation and dissolution processes of A 6061-T6 under different temperatures. It is known that the supersaturated solid solution of Al-Mg-Si alloys decompose as follows: Al supersaturated solid solution (SSSS) → Mg-Si phase clusters → Guinier Preston (GP) zones, enriched in Si and Mg → needle-shaped β″ (Mg_5Si_6) precipitates → rod-shaped β′ precipitates → equilibrium disk-shaped platelets β(Mg_2Si) with a face cubic centered structure [14,15]. In its initial high strength T6 condition, Al-Mg-Si alloys contain a large density of β″ precipitates, which dissolve in the stir zone and depending on their size are dissolved (smaller ones) or transformed into large β′ precipitates (bigger ones) in heat affected zone, which leads to significant reduction of precipitation density [14]. All these transformations are connected to certain temperature ranges: at temperature above 220–250°C dissolution of small strengthening precipitates β″ (Mg_5Si_6) and the growth of large β″ occurs; the rise of temperature from 250 to 320°C leads to transformation of large β″ to β′; at 400–480°C the β′ phase dissolute and at 480-502°C the precipitation and dissolution of β takes place [15,16]. In current investigation maximum temperature is measured to be 350-400°C for both straight and cycloid-like welding trajectory, which lead to the conclusion that some β′ and/or β precipitates may be present in the nugget zone. So, it is obvious that the heat input has major role in determining the microstructural evolution and mechanical properties of the friction stir welded materials [17]. The most significant deterioration in strength

characteristics is observed for the “S” series material due to the used cycloid-like welding trajectory which leads to longer exposure of welding bed at higher local temperatures and thus dissolution of bigger amount of strengthening precipitates. It is also visible, that stir friction welding by cycloid-like trajectory leads to homogenization of the material in welded zone and thus to higher plasticity than series “V”. In fact, series “S” specimens produced with cycloid-like trajectory have more stable strength characteristics, lower strength and higher ductility.

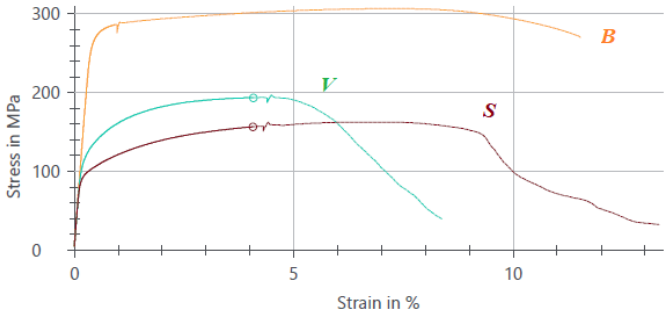

Fig. 11. Tensile testing of specimens of the base material A6061 T651 (line B) and FS welded specimens series “V” and “S “

4.3 Visual fractography

The specimen fracture of series “V” (Fig. 12 and 14) and series “S” (Fig. 13 and 15) illustrate the differences between the two types FSW by linear motion of the tool and motion on a cycloid-like trajectory. The presence of individual defects is the reason for the unstable strength properties of FSW specimens.

The FSW process is accompanied by the formation of microcracks, which grow into cracks when the load increases. In series “V” only one crack is observed (Fig. 13), while in series “V” a few cracks are observed (Fig. 14) with plastic zones between them. In the series “S” specimens the cracks are at a distance equal to the processing step.

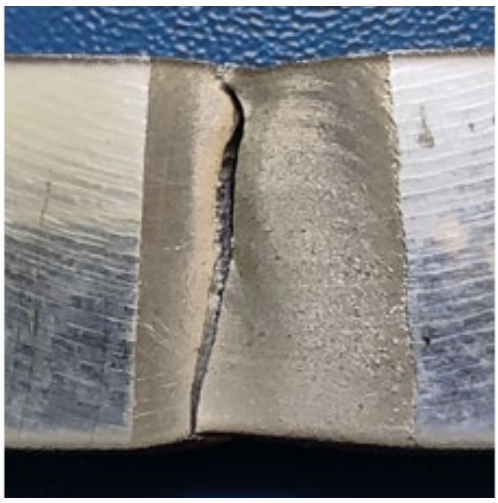

Fig.12. Fracture of specimen series “V”

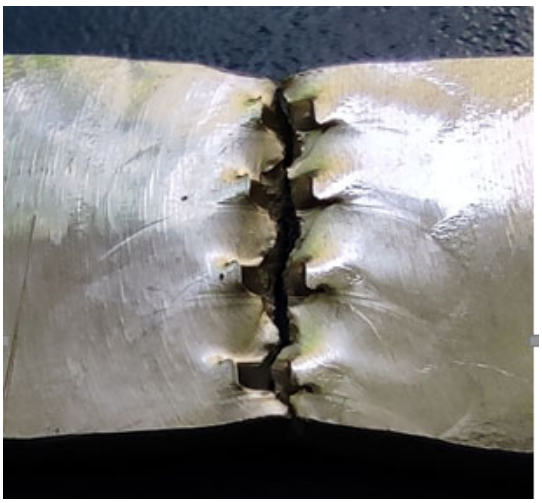

Fig.13. Fracture of specimen series “S”

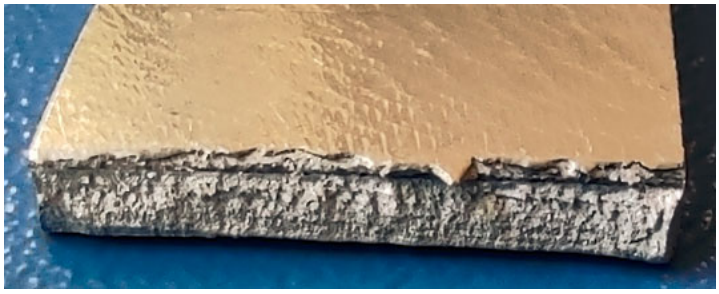

Fig.14. Fracture of specimen series “V”

Fig.15. Fracture of specimen series “S”

5. Conclusions

The mechanical properties of the weld joints in two types of FSW are studied and compared with the base material. The tensile strength of both welds is reduced (Fig.11). The decrease in strength characteristics is mainly due to the thermal impact in the process of FSW, which worsens the effect of heat treatment. In FSW with a cycloid-like trajectory, the strength is the lowest, which means that the mentioned impact is the strongest. The strength properties of the welds in FSW can be optimized through decreasing the step of processing, changing the type of trajectory and the parameters of the processing.
The friction stir processing (FSP) with cycloid-like trajectory of the tool moving could result in better stirring of the reinforcing powder to obtain nonequilibrium hybrid composites and would eliminate the need for multi-pass processing.

Acknowledgements

The authors thank the National Research Fund for the financial support provided through the contract KP-06-India 10/02.09.2019 and the European Regional Development Fund, Operational Program "Science and Education for Smart Growth 2014-2020", CoE Project "National Center for Mechatronics and Clean Technologies” BG05M2OP001-1.001-0008.

References

1. R.S. Mishra, Z.Y. Ma, Friction stir welding and processing, Mater. Sci. Eng. R 50 (2005) 1–78.
2. Ch. Radhika, N. Shyam kumar.;" Process Parameters Optimization of Aa2024 Alloy Friction Stir Welding using Taguchi's Technique." International Journal of Innovative Technology and Exploring Engineering 8 (2019) 1940-45.
3. N. Ferdinandov, D. Gospodinov, Peculiarities and Application of Friction Stir Welding, International Journal "NDT Days", Volume IV, Issue 3, Year 2021
4. Rambabu, P.; Prasad, N.E.; Kutumbarao, V.V.; Wanhill, R.J. Aluminium Alloys for Aerospace Applications. Aerospace Mater. Mater.Technol. 2017, 1, 29–52.
5. Velaphi Msomi et al., Al-Based Surface Composites and Strengthening of Welded
6. Joints Through Multi-Pass FSP Technique, International Journal of Advanced Trends in Computer Science and Engineering, 10(2), March – April 2021, 1426 – 1440
7. Elvira Wahyu Arum Fanani, Eko Surojo Recent Progress in Hybrid Aluminum Composite: Manufacturing and Application, Metals 2021, 11, 1919
8. Gandra, J., Vigarinho, P., Pereira, D., Miranda, R.M., Vilac¸ a, P., 2013.Wear characterization of functionally graded Al-SiC composite coatings produced by friction surfacing. Mater. Design 52, 373–383, http://dx.doi.org/10.1016/j.matdes.2013.05.059.
9. Ahat Samadi Welding defects formation and the effect of FSW parameters on them,2011
10. Marie F., Alléhaux D., Esmiller B. Development of the bobbin tool technique on various aluminum alloys. In: 5th Int. Symp. Frict. stir Weld., Metz, France; 2004.p. 39–52.
11. Amir Hossein Baghdadi, Zainuddin Sajuri at al." Mechanical Property Improvement in Dissimilar Friction Stir Welded Al5083/Al6061 Joints: Effects of Post-Weld Heat Treatment and Abnormal Grain Growth", Materials (Basel), 2021Dec31;15(1).
12. Cabibbo, M.; Forcellese, A.; Simoncini, M. New Approaches to the Friction Stir Welding of Aluminum Alloys in Joining Technologies; InTech: Rijeka, Croatia, 2016; Chapter 2.
13. Ramanjaneyulu K., Madhusudhan Reddy G., Venugopal Rao A. and Markandeya R. Structure-Property Correlation of AA 2014 Friction Stir Welds: Role of Tool pin profile, Jurnale of Maretials Engineering and Performance 22 (8), DOI:10.1007/s11665-013-0512-4
14. Heidarzadeh, A., Mironov, S., Kaibyshev, R., Çam, G., Simar, A., Gerlich, A., Khodabakhshi, F., Mostafaei, A., Field, D.P., Robson, J.D., Deschamps, A., J. Withers, P. Friction stir welding/processing of metals and alloys: A comprehensive review on microstructural evolution. Progress in Materials Science 117 (2021) 100752, https://doi.org/10.1016/j.pmatsci.2020.100752
15. Abioye, T.E., Zuhailawati, H., Anasyida, A.S., Yahaya, S.A., Dhindaw, B. K. Investigation of the microstructure, mechanical and wear properties of AA6061-T6 friction stir weldments with different particulate reinforcements addition, Journal of Materials Research and Technology, Vol. 8, Issue 5, 2019, pp 3917-3928, ISSN 2238-7854, https://doi.org/10.1016/j.jmrt.2019.06.055.
16. Peng Dong, Daqian Sun, Hongmei Li, Natural aging behaviour of friction stir welded 6005A-T6 aluminium alloy, Materials Science & Engineering A 576 (2013) 29–35, http://dx.doi.org/10.1016/j.msea.2013.03.077
17. Ma, Z. Y., Feng, A. H., Chen, D. L., Shen, J. (2017) Recent Advances in Friction Stir Welding/Processing of Aluminum Alloys: Microstructural Evolution and Mechanical Properties, Critical Reviews in Solid State and Materials Sciences, http://dx.doi.org/10.1080/10408436.2017.1358145